Howard Hughes Medical Institute

Published as: *Neuron*. 2016 December 07; 92(5): 1079–1092.

Coding and plasticity in the mammalian thermosensory system

David A. Yarmolinsky[1], **Yueqing Peng**[1], **Leah A Pogorzala**[2], **Michael Rutlin**[1], **Mark A. Hoon**[2], and **Charles S. Zuker**[1]

[1]Howard Hughes Medical Institute and Departments of Biochemistry and Molecular Biophysics and of Neuroscience, Columbia College of Physicians and Surgeons, Columbia University, New York, NY 10032, USA

[2]National Institute of Dental and Craniofacial Research, National Institutes of Health, Bethesda, MD 20892, USA

Summary

Perception of the thermal environment begins with the activation of peripheral thermosensory neurons innervating the body surface. To understand how temperature is represented *in vivo*, we used genetically-encoded calcium indicators to measure temperature-evoked responses in hundreds of neurons across the trigeminal ganglion. Our results show how warm, hot and cold stimuli are represented by distinct population responses, uncover unique functional classes of thermosensory neurons mediating warm and cold sensing, and reveal the molecular logic for peripheral warmth sensing. Next, we examined how the peripheral somatosensory system is functionally reorganized to produce altered perception of the thermal environment after injury. We identify fundamental transformations in sensory coding, including the silencing and recruitment of large ensembles of neurons, providing a cellular basis for perceptual changes in temperature sensing, including heat hypersensitivity, persistence of heat perception, cold hyperalgesia, and cold analgesia.

Introduction

Descartes, in his classic depiction of heat sensation over 350 years ago, proposed a direct link between “particles of heat” and the brain(Descartes et al., 1644). Our current understanding of mammalian thermosensation is shaped, on the one hand, by anatomical, psychophysical, and electrophysiological experiments, and on the other, by the cloning and characterization of genes encoding temperature sensitive ion channels. Studies beginning nearly a century ago demonstrated the existence of diverse cutaneous nerve endings sensitive

Lead Contact: Charles Zuker/ cz2195@columbia.edu.

Author Contributions

DAY developed the imaging preparation and experimental platform, and carried out all imaging studies. YP developed the behavioral studies to study warmth sensing, LAP engineered the Trpm8^{cre} transgenic line, and helped with behavioral experiments. MR carried out expression studies on the various reporter lines. DAY, MAH and CSZ conceived and designed experiments, analyzed data, and wrote the manuscript.

to cooling or heating. These include both dedicated thermosensors as well as polymodal neurons activated by thermal, mechanical, and/or chemical stimuli (Schepers and Ringkamp, 2009). A transformative advance in our understanding of pain and thermosensation came with the seminal discovery of a set of members of the TRP family of ion channels activated by both chemical irritants and temperature(Julius, 2013). The founding member of the 'thermo-TRP' family, TRPV1, is the most thoroughly characterized mammalian heat sensitive ion channel, and is gated *in vitro* by heating with an activation threshold close to the psychophysical threshold for thermal pain (~43° C)(Caterina et al., 1997). Additional thermally gated channels expressed by sensory neurons include TRPM8 (generally known as the "menthol receptor", and a cold-sensitive channel (McKemy et al., 2002; Peier et al., 2002)), TRPA1 (generally known as the "wasabi receptor"(Jordt et al., 2004; Story et al., 2003)), TRPV2 and TRPM3 (channels gated by extreme heat)(Caterina et al., 1999; Vriens et al., 2011).

The 'thermoTrp tiling' model of thermosensation posits that expression of different thermosensitive TRP channels in primary sensory neurons endows diverse populations with distinct thermal sensitivities(McKemy et al., 2002; Saito and Tominaga, 2015). Several studies applying mouse molecular genetics have demonstrated this principle to be broadly correct. For example, ablation of sensory neurons expressing Trpm8, a cold-activated channel(McKemy et al., 2002), leads to a profound loss of cold sensation(Knowlton et al., 2013; Pogorzala et al., 2013), while ablating or silencing neurons expressing the heat-sensing channel TrpV1 results in a corresponding loss of heat avoidance to temperatures as high as 50° C (Cavanaugh et al., 2009; Pogorzala et al., 2013). Thus, these channels mark cell types that operate as labeled lines for hot and cold detection.

Importantly, beyond this broad division, the cellular and molecular basis of thermosensory coding has remained elusive. For instance, the roles of channels previously proposed to mediate innocuous warmth sensing (TrpV3 and TrpV4 (Guler et al., 2002; Xu et al., 2002)) and noxious cold sensation (TrpA1 (Story et al., 2003)) have been called into question by *in vivo* studies (Huang et al., 2011; Pogorzala et al., 2013). Similarly, while TrpV1 is frequently cited as the key mediator of thermal pain for noxious heat (e.g. >43° C) (Vriens et al., 2014), mice lacking the TrpV1 channel have only modest defects in detecting and responding to high temperatures under normal conditions(Caterina et al., 2000; Davis et al., 2000; Pogorzala et al., 2013). In contrast, TRPV1 plays an indispensible role in the plasticity of thermal sensation. The most salient phenotype of TrpV1 null mice is a profound loss of the thermal hypersensitivity normally associated with inflammation(Caterina et al., 2000; Davis et al., 2000). Notably, the TRPV1 channel itself can be dramatically sensitized to temperature by post-translational modification, providing a molecular mechanism for heat hyperalgesia and allodynia (Julius, 2013; Tominaga et al., 1998; Vellani et al., 2001).

How do genetically specified populations of thermosensors generate a cellular representation of temperature *in vivo*, and how does this representation change to produce altered thermal perception? Here, we have applied *in vivo* calcium imaging using genetically encoded calcium indicators to visualize the representation of temperature at the level of molecularly defined neuronal ensembles. Our results reveal how thermal stimuli are represented *in vivo*, provide distinct roles to defined classes of thermosensory neurons, uncover the cellular and

molecular basis for innocuous warmth sensing, and demonstrate how functional plasticity at the periphery can provide a substrate for transformation of thermal perception.

RESULTS

We developed an *in vivo* calcium-imaging platform that allowed us to optically record activity from large ensembles of genetically marked somatosensory neurons. To target a genetically encoded indicator of activity to selected neurons, we made use of an engineered mouse line that expresses the GCaMP5A calcium reporter (Akerboom et al., 2012) under the control of a Cre-dependent CAG promoter from the Rosa26 locus (see Methods). Crossing this line to specific Cre drivers permitted either pan-neuronal or genetically restricted labeling of somatosensory neurons with GCaMP5 (Fig. 1A). To label all somatosensory neurons with the GCaMP reporter we used a $Wnt1^{Cre}$ driver line (Lewis et al., 2013), and to selectively label the repertoire of neurons required for thermosensory behaviors we used $TrpV1^{Cre}$ ($TrpV1^{Cre}$ functions as a lineage tracer reporter, marking all classes of hot and cold sensing neurons; see (Mishra et al., 2011)). We also generated additional mouse lines to label unique sub-classes of somatosensory neurons, including those defined by $Trpa1^{Cre}$ and $Trpm8^{Cre}$.

Imaging temperature-evoked responses *in vivo*

To study thermosensory coding we focused on the trigeminal ganglion, the primary relay for somatosensory information from the head, face, and mouth. As the trigeminal ganglion is by far the largest of the somatosensory ganglia, this *in vivo* preparation affords sampling of thousands sensory neurons in single animals. We chose the oral cavity to analyze temperature coding, as it is densely innervated by thermosensory afferents, it is readily accessible to pharmacological agonists of thermoTRP channels (e.g. capsaicin, menthol and mustard oil), and it provides a large receptive surface that can be effectively probed with a controlled thermal stimulus.

For functional imaging *in vivo*, we developed a preparation that exposed the full extent of the trigeminal ganglion surface (Fig. 1B,C), and localized the neurons representing the oral cavity by examining responses to mechanical and thermal stimuli across the mouth and face while imaging the ganglion. Our results demonstrated that most neurons innervating the oral cavity are localized to the medial-lateral surface of the ganglia (i.e. at the entrance of the mandibular nerve; Fig. S1); this region became the focal point of our imaging studies.

We delivered defined thermal stimuli by perfusing the oral cavity with a constant stream of water circulated through a high-sensitivity Peltier-controlled temperature modulator (see Fig 1B). To characterize thermosensory representation at a global level, we measured responses to a graded series of temperature steps, ranging from 5° to 50° C in animals expressing GCaMP under the control of $TrpV1^{Cre}$ and $Wnt1^{Cre}$ (see Methods for details). For both genotypes, we observed robust, widespread, and selective calcium responses to thermal stimuli (Fig 1D). Responses were highly reliable and stimulus-dependent (Fig. S2), and the imaging preparation was stable over several hours (see Methods for details).

To validate this platform as a faithful representation of peripheral thermosensory activity, we first asked whether the preparation recapitulates the functional segregation of hot- and cold-sensing neurons [3]. As expected, the vast majority of neurons responded selectively: from over 800 thermosensory neurons analyzed for responses to our full panel of temperature steps (Fig S2), more than 90% responded specifically either to heating or to cooling (distribution of temperature responses was nearly identical between Wnt1 and Trpv1^{Cre} driver lines, Fig S2F). Thus, the nature of thermal stimuli is primarily encoded in labeled-line fashion, by selectively tuned thermosensors(Cavanaugh et al., 2009; Julius, 2013; Knowlton et al., 2013; Palkar et al., 2015; Pogorzala et al., 2013). These cold and hot neurons are intermingled, with no evidence for clustering or topographic organization by modality (see Fig. 1D). Notably, we also reliably detected a small fraction of neurons (37/837) that respond bimodally to temperature stimuli (e.g. Fig. 1E, bottom trace). Such neurons may signal the presence of thermal danger(Frank et al., 2015).

Functional and molecular logic of heat and warmth sensation

How do peripheral sensory neurons represent innocuous warmth versus noxious heat? We imaged the population responses to stimulation with temperatures between 33° C and 53° C. A given temperature activated an ensemble of neurons distributed throughout each imaging field (Fig 2A,B); the responses were consistent and robust, and there was no evidence for topography or patterning (see Fig S4). Different temperatures generated distinct representations (compare different panels in Fig. 2C and Fig S3), with the vast majority of neurons responding only to noxious temperatures (> 43° C, referred to as ‘heat’ or noxious heat neurons). Notably, in every ganglion we could also identify a much smaller population (~10% of heat-responding cells, here referred to as warmth sensors) exhibiting exquisitely sensitive responses to warming (Fig. 2A–D). These neurons reliably responded for over an hour of repeated stimulation with mild warming pulses (Fig. S3). Warmth-sensing neurons were intermingled with noxious heat neurons, with no discernible spatial organization (see Fig 2A and Fig S3).

By examining the temperature preferences and response amplitudes of the warm and noxious heat neurons at different temperatures, we could discern how together they produce unique representations to encode temperature *in vivo*. Our results demonstrated that warmth-sensing neurons exhibit graded responses to changes in temperature intensity, have a broad dynamic range, and respond from innocuous warm to over 50° C (Fig 2D–H). In contrast, noxious neurons have a very narrow dynamic range (see Fig 2D–E); higher temperatures recruited more noxious neurons (compare panels in Fig 2C and S4) and evoked larger responses, but they quickly reached maximal amplitudes and saturated within a few degrees (see Fig 2D). Thus, warm sensors, although only a small fraction of the total population, likely play a critical role in representing the quality of a thermal stimulus, while the noxious sensors act in essence as binary switches for painful temperatures. Collectively, these results illustrate how population responses can distinctively represent differences between warm, mildly hot, and noxious stimuli.

TRPV1 and the neurons that express TRPV1 are widely ascribed the function of noxious heat sensors(Palkar et al., 2015; Vriens et al., 2014). In contrast, although innocuous warmth

sensation is critical for maintenance of thermal homeostasis, the cellular and molecular basis of this modality has remained poorly understood (Huang et al., 2011), largely due to the relative scarcity of warmth sensing neurons. To probe the molecular identity of the warmth and noxious heat neurons, we first stimulated the oral cavity with warm and noxious temperatures, and then with the TRPV1 specific agonist capsaicin. As expected, the majority (>70%) of noxious heat sensors expressed TrpV1 ((Cavanaugh et al., 2009; Pogorzala et al., 2013), Fig S3). Surprisingly, these experiments also revealed that the entire population of warmth sensors uniformly expresses TrpV1; all warmth neurons displayed clear capsaicin responses (Fig S3, see also Fig 2F,H). In fact, no other type of neuron was found to respond to warm stimuli *in vivo* (see (Tan and McNaughton, 2016)). Thus, warmth-sensing neurons represent a novel and functionally distinct class of TrpV1-expressing sensory neurons. Given the unexpected segregation of Trpv1-expressing neurons into noxious- versus warmth temperature sensing, we next asked: what is the role of the TRPV1 channel itself in mediating these two types of responses?

Acute inactivation of TRPV1 should reveal its requirement, and therefore we examined the responses of functionally identified noxious and warmth sensors before and after blockade of TRPV1 channel function with the selective TRPV1 antagonist JNJ-17203212 (Swanson et al., 2005). We found that inhibition of TRPV1 had only a small effect on the overall representation of noxious heat responses (Fig S4A–C). For example, at the moderately noxious temperature of 48° C, approximately 75% of the noxious heat-sensing neurons still retained robust responses, and at 52° C over 90% retained heat responses even after TrpV1 inhibition (Fig. S4C). These results are consistent with the minor behavioral effect of TrpV1 knockout on heat responses(Davis et al., 2000; Pogorzala et al., 2013), and demonstrate that at the level of peripheral coding, TRPV1 makes only a limited contribution to the normal representation of noxious heat.

What about warmth detection? In contrast to the minor deficit seen on noxious heat sensing upon Trpv1 channel inactivation, application of the TRPV1 antagonist completely eliminated warmth responses (35–43° C) (Fig. 3A, B). Thus, we reasoned that warm responses *in vivo* should be abolished in TRPV1 knockout animals. We therefore generated and imaged responses in mice homozygous null for TrpV1 and expressing GCaMP5 in all neurons. Indeed, our results demonstrated that responses to innocuous warmth (below 43° C) were entirely absent in TrpV1 knockouts (Fig. 3C–D). As anticipated, these mutant animals still retained significant and widespread responses to noxious heat, while exhibiting the expected loss of responses to capsaicin (see Fig. 3C right panel).

An important prediction of these results is that inhibition of TRPV1 should significantly affect the ability of animals to sense and respond to warm temperatures. We developed a behavioral test where motivated animals (i.e. thirsty) were instructed to sample and discriminate between warm (40° C) and room temperature (RT, 32° C) stimuli. In this assay, thirsty animals were trained to sample a thermally-controlled central spout, and then to report its temperature by poking into a right or a left port (a correct response was given a water reward; see Methods for details). This learned behavior requires that the animal samples the spout, recognizes its temperature and executes the appropriate behavior in each trial. After 40 sessions of training (each with 80 randomly presented 32° C or 40° C stimuli),

mice were able to report the probe's temperature with near 90% accuracy. Figure 3E demonstrates that, as hypothesized, inhibition of TRPV1 severely impaired warm temperature detection (see figure legend for details). Importantly, animals still retained their strong aversive responses to noxious heat (Fig. S4 D–E), and their deficit in warm temperature sensing was fully reversible upon washout of the drug (data not shown). Taken together, these results recast the role of TrpV1 *in vivo* as an essential molecular mediator of warmth responses.

Functional and molecular logic of cold sensation

The experience of cold encompasses a wide variety of sensations, ranging from pleasantly cool to excruciatingly painful. How is the spectrum of cold temperatures represented *in vivo*?

We imaged responses to a broad range of cold temperatures, from innocuous to noxious cold. Each temperature activated a significant population of neurons in the imaging field, with the most common type (here referred to as Type I), representing approximately 70% of all cold sensors (Fig. 4A–B). Type I cold sensors responded tonically to mild cooling but quickly inactivated when temperature dropped below the innocuous range (~20° C; Fig 4C–D); these are hallmarks of the classically defined cold receptors (Hensel and Zotterman, 1951; Schepers and Ringkamp, 2009) (see Fig S5 for a larger sampling of temperatures). Although the activity of type I neurons can robustly signal mild cooling temperatures (>20° C), given their rapid silencing during persistent noxious cold we wondered what sensory populations allow the organism to remain responsive to noxiously cold temperatures?

Two novel functional classes of cold-sensing neurons account for the peripheral representation of intense cold. One population, referred to as Type II, and defining approximately 20% of cold-sensing neurons, responded with sustained activity even at extremely noxious cold temperatures (<10° C; Fig 4); this class is ideally suited to encode intense cold. An additional, rare class (Type III, representing <10% of the total population of cold sensors) exhibited a hybrid response profile, behaving like type I cells within the mild to moderate range but producing a secondary, non-adapting response upon exposure to intense cold, that sometimes persisted even beyond removal of the cooling stimulus (see Fig 4C).

What are the molecular identities of these functionally diverse cold-sensing neurons? Two members of the TRP family of ion channels have been linked to cold sensation, and have been suggested to define distinct classes of cold sensing neurons: Trpm8 for innocuous or moderate cooling, and TrpA1 for noxious cold (McKemy et al., 2002; Story et al., 2003). Mice lacking Trpm8 exhibit a clear and selective loss of innocuous cold sensation (Bautista et al., 2007; Colburn et al., 2007; Dhaka et al., 2007). In contrast, the role of TrpA1 for cold sensing *in vivo* is unclear; behavioral analyses of knockout mice have reported either deficient or normal noxious cold sensation (Bautista et al., 2006; Karashima et al., 2009; Kwan et al., 2006). Thus, we engineered mice expressing GCaMP5 under the control of TrpA1 or Trpm8 regulatory elements and examined the roles of each population in cold sensing (see Fig. S6 and Methods).

Our results showed that Trpm8^{Cre} marked all 3 classes of cold sensing cells (Fig. 4D). In contrast, the population defined by TrpA1^{Cre}, although strongly responsive to stimulation with the TrpA1 ligand AITC (Fig. S6), was essentially insensitive to cold; even extreme cold stimulation (1° C) failed to evoke an appreciable response (Fig. 4E, bottom left panel). In contrast, TrpA1 neurons exhibited robust and selective responses to heat (Fig 4E and Fig S6). In fact over 95% of the TRPA1-positive neurons that responded to temperature stimuli were activated by heat, while less than 1% displayed any activity to cold (Fig S6 panel C); these results are consistent with the observation that TrpA1-expresing neurons are a subset of TrpV1-expressing neurons (Pogorzala et al., 2013; Story et al., 2003). Therefore, we reasoned that ablation of the TrpA1-expressing neurons would have no effect on behavioral avoidance of cold, but should impact noxious heat avoidance. Indeed, our results showed both postulates to be correct (Fig. S6), substantiating TrpA1-expressing neurons as functioning in heat rather than cold sensing.

These results demonstrate that Trpm8 neurons comprise distinct functional classes encompassing the broad range of physiologically relevant cold stimuli, from mild to noxious, and showed how, at a population level, Type I, II and III cold-sensing neurons can generate unique representations to collectively encode cold *in vivo*.

Plasticity in temperature coding after heat injury: Ongoing pain after injury and cold analgesia

The perceptual quality and behavioral valence of a fixed thermal stimulus can vary widely based on context and internal state. Here, we explored the plasticity of thermosensory coding by examining the consequences of heat-induced injury, a natural and physiologically relevant insult that rapidly induces changes in thermal perception. A salient sensory consequence of burn injury (and other pain conditions) is the ongoing perception of “burning” pain at normal skin temperatures, long after the damaging stimulus is gone. How does the representation of temperature change to produce such altered perception? The capability to monitor activity for extended periods across somatosensory populations *in vivo* provided a unique opportunity to examine this phenomenon, and ask if basal spontaneous activity across peripheral populations is indeed altered by injury.

First, we mapped the representation of warm-, heat- and cold-sensing neurons in the ganglia by recording responses to a graded series of temperature stimuli from 4° C to 50° C. Then, we analyzed patterns of activity at a neutral temperature of 32° C, before and after a 15 second heating pulse at 55° C pulse to induce injury. Our results (Fig. 5A,B) uncovered a dramatic increase in spontaneous activity across all imaging fields that persisted for several minutes after termination of the 55° C injury-inducing pulse; this activity could be either sporadic or continuous over time (e.g. Fig 5B). Notably, the majority of spontaneously active neurons were noxious heat sensors (Fig. 5C).

A remarkable feature of ongoing pain following burn is that it can be significantly alleviated by cooling; this is one of the oldest known analgesic therapies (Evans, 1981). This effect has been suggested to rely primarily on central inhibition of pain by stimulation of cold sensing neurons(Proudfoot et al., 2006). However, given our identification of candidate neural targets for ongoing/persistent pain at the periphery, we wondered whether cooling might

directly inhibit ongoing activity by acting on these neurons. To test this idea, we specifically examined the effect of mild cooling on the activity of noxious heat sensing neurons after injury. Indeed, our results demonstrated that injury-induced activity is strongly and reversibly suppressed by cooling (**Panel 5D,E**). Together, these results identify a cellular basis for persistent pain after burn injury, and substantiate a critical role for peripheral mechanisms in mediating cold analgesia.

Transformation of temperature representation

Changes in temperature perception after insult, injury or pathology play an important, and significant role in protecting tissue from further damage. A familiar example is the rapid shift in temperature perception after burn, where normally innocuous warm stimuli can become extremely painful. How does the representation of temperature change to transform perception?

A number of elegant studies using genetic and pharmacological tools have shown that the TRPV1 channel is critically required for the induction of chemical- and inflammation-induced heat hypersensitivity(Caterina et al., 2000; Chuang et al., 2001; Davis et al., 2000). Here, we wished to investigate how such insults modify the cellular representation of heat at the level of peripheral populations(Julius, 2013). We examined responses to a graded series of heating stimuli from 36° C to 50° C, mapped their representation in the ganglia, provided a 15 second heating pulse at 55° C to induce injury, and then re-mapped responses to the same stimulus series.

Figure 6A shows that after thermal injury there is dramatic expansion in the population of neurons responding to warmth, with dozens of new neurons recruited in each imaging field after injury (e.g. the sample field shown in Fig 6A displays a single neuron responding to warm stimuli prior to injury, but dozens after). To determine how this expanded representation is generated (i.e. where are these previously undetected responses to warm temperature coming from?), we examined the temperature selectivity of sensitized neurons prior to injury.

Our results (Fig. 6B,C) demonstrated that the responses emerging after heat injury could be explained entirely by a shift in the thermal sensitivity of noxious heat sensors into the normally innocuous range. In fact, we did not detect any de novo emergence of heat sensitivity from previously ‘silent’ neurons (i.e. all sensitized neurons responded to noxious heat stimuli prior to injury). Significantly, the responses of warmth neurons were unchanged (e.g. Fig 6D). Given the essential requirement for TRPV1 in chemical- and inflammation-induced heat hypersensitivity (Caterina et al., 2000; Chuang et al., 2001; Davis et al., 2000), we reasoned TRPV1 should also mediate burn injury-induced sensitization. Indeed, pharmacological blockade of TRPV1 abolished the warmth responses in sensitized neurons after burn injury(Fig 6D–E). These results confirm the indispensable role of TRPV1 in mediating heat allodynia, and provide a population view of the transformation of thermosensory coding after injury, illustrating how and why normally innocuous warm stimuli may have such a dramatic impact in pain perception after thermal insult.

Transformation of cold sensation

How is the coding of cold temperature transformed by injury? We examined responses from 30° C to less than 5° C, determined their representation in the ganglia, gave a heating pulse at 55° C to induce injury, and then re-examined the representation of the same stimulus series. Remarkably, thermal injury leads to a dramatic loss of the representation of cold, with the majority of type I cold sensors now unresponsive (Fig. 7). Given that type I cold sensors comprise the majority of cold sensing neurons, this transformation would radically change cold temperature coding, probably explaining deficits in cooling sensation upon burn injury(Pedersen and Kehlet, 1998). Importantly, the responses of type II cold sensors are unaffected (Fig 7B), thus preserving the capacity for noxious cold detection.

When we compared the set of neurons activated by cold before and after injury we also uncovered a population of cold sensing neurons that only emerges following injury (Fig. 8A). These neurons are completely silent to all thermal stimuli prior to injury (therefore defined here as “silent thermosensors”), yet after injury signal strongly when stimulated with cold temperatures (Fig. 8B). Unlike all other classes of cold neurons, these silent thermosensors respond transiently at all stimulus intensities (Fig. 8C, D). Thus, these neurons are activated at the onset of cooling stimuli (for example upon contact with a dangerously cold surface).

What is the molecular identity of the silent thermosensors? We directly tested $Trpm8^{Cre}$; GCaMP responses to cold before and after thermal injury. Figure 8E (left panel) shows that silent thermosensors are a subset of the $Trpm8^{Cre}$ population. Furthermore, these neurons co-express CGRP (Figure S7), a marker for peptidergic nociceptors (McCoy et al., 2013). Thus, the recruitment of silent thermosensors after injury is likely to mediate pain in response to stimulation by cold, and therefore we hypothesized that there would be an enhancement of behavioral sensitivity to cold after thermal injury. We used a plantar withdrawal behavioral assay(Brenner et al., 2012) to compare the nocifensive response of mice to cold in normal and injured states. As predicted, mild burn injury induces a robust behavioral sensitization to cooling, of magnitude comparable to inflammatory and neuropathic treatments(Brenner et al., 2012) (Fig. 8F). Together, these results define silent thermosensors as a novel class of neurons that may serve as the cellular substrate for cold allodynia.

Concluding Remarks

By stimulating and recording from large populations of genetically defined neurons in live animals, we were able to comprehensively assess the representation and the logic of temperature coding at the periphery. This approach preserved the biological integrity of the thermosensory system, and provided the first global view of how temperature is represented in the activity of somatosensory neuronal populations.

A number of unanticipated findings emerged from this study: (1) the identification of TRPV1-expressing neurons as the principal innocuous warm detectors; (2) the demonstration that the TRPV1 channel itself is indispensable for peripheral warm sensing, (rather than noxious heat detection); (3) the separation of cold sensing into at least 3

functionally distinct classes of TRPM8-expressing neurons; (4) the extraordinary large-scale desensitization of Type I cold sensors after burn injury as one of the most dramatic widespread sensory transformations following thermal injury; (5) the emergence of silent thermosensors after cold injury, and 6) demonstrating TRPA1-neurons as functioning in hot rather than cold sensing (and remain completely unresponsive to cold stimuli, even in the injured state; see Fig 8E)

Our results showed how injury transforms the cellular representation, coding logic and behavioral responses to thermal stimuli. For heating, we showed how TrpV1-expressing noxious heat-sensing neurons produce a re-mapping of temperature representation following injury *in vivo*. While the normal heat-sensing function of these cells is largely independent of TRPV1, these same neurons become dependent on TRPV1 for thermal hypersensitivity after injury(Caterina et al., 2000; Davis et al., 2000). Given the essential role of TRPV1 in normal warmth sensing (Fig 3), we suggest that the sensitization of noxious sensors may reflect functional modifications in the TRPV1 ion channel that mimic its state in warmth-sensing cells (see (Vellani et al., 2001)). A recent study reported that TRPM2 functions as a warm sensor *in vitro* in dissociated dorsal root ganglion and sympathetic neurons(Tan and McNaughton, 2016). However, we find no evidence for any neuron, other that TRPV1-expressing, as functioning as peripheral warm sensors *in vivo,* in the intact preparation.

The discovery of a class of silent cold sensors that emerges after injury may provide a novel mechanism for cold-induced pain, a major complication of many inflammatory and neuropathic conditions (Verdugo and Ochoa, 1992). In contrast to heat hypersensitivity, where the tuning of existing noxious heat sensors is altered, this transformation involves functional recruitment of a new class of cold-sensing neuron. Molecular identification of this population provides an avenue to examine their role in clinically relevant models of cold allodynia, and to determine the cellular and molecular mechanisms underlying the switch between silent and active sensing states.

In the future, it will be exciting to take advantage of developing platforms for whole brain imaging studies to decipher how peripheral and central circuits come together to orchestrate thermal homeostasis, behavioral actions, and perception, and in what way central circuits for temperature and pain change in response to pathological conditions and disease.

MATERIALS AND METHODS

Transgenic animals

All procedures involving animals followed US National Institutes of Health (NIH) guidelines for the care and use of laboratory animals, and were approved by the Columbia University or National Institute of Dental and Craniofacial Research Animal Care and Use Committees. TrpV1^{Cre}, Wnt1^{Cre} and TrpV1 knockout mice have been described previously; Wnt1^{Cre} serves as a lineage marker for essentially all (>90%) of somatosensory neurons, TrpV1^{Cre} labels a large subset (>50%) that are required for innate thermosensory behaviors (Caterina et al., 2000; Lewis et al., 2013; Mishra et al., 2011). Trpm8^{Cre} mice were generated by recombineering of BAC RP24-78N24. GFP-2A-Cre was inserted in frame at the initiation codon of Trpm8. Trpa1-Diphtheria Toxin Receptor-2A-Cre mice were

generated by inserting the bi-cistronic cassette at the start codon of the endogenous Trpa1 locus. Rosa26^{GCaMP5} mice were a generous gift from Nick Ryba and were generated by inserting the coding sequence for GCaMP5A into the Rosa26 locus following a loxP flanked STOP cassette. For imaging, TrpV1 knockout mice and wild type mice were crossed to Rosa26^{GCaMP} mice in which the STOP cassette was excised in the germline (ΔRosa26^{GCaMP}), resulting in ubiquitous reporter expression including all trigeminal neurons. Supplementary Table 1 lists the genotypes, gender, age and sex of animals used in this study.

Surgical preparation

The surgical approach was adapted from a method previously reported (Rothermel et al., 2011). Mice were anesthetized with ketamine and xylazine (100 mg/kg and 10 mg/kg intraperitoneal) with booster doses administered as necessary to maintain surgical plane anaesthesia. Core body temperature was maintained at 36±1° C with a closed loop heating system throughout surgery and imaging. Mice were tracheotomized to allow breathing during oral stimulus presentation. The head was stabilized by affixing a stainless steel bar to the skull with cyanoacrylate followed by dental acrylic. A unilateral craniotomy, followed by hemispherectomy, was performed to obtain optical access to the dorsal surface of trigeminal ganglion.

Calcium imaging and thermal stimulation

For thermal stimulation, a stimulus tube was placed inside the oral cavity for continuous perfusion at ~0.5ml/second with deionized water passed through digitally controlled peltier chiller/heater units (TE Technology). To deliver thermal stimuli, a valve controller (Biologic) was used to switch flow from a baseline source held at constant temperature (32° C) to a stimulus source generating hot or cold thermal pulses. Intra-oral temperature was continuously monitored using a digital thermometer electronically synchronized to image acquisition (Vernier Software & Technology). Oral temperature was held at 32° C at all times between imaging trials, and all thermal stimuli were interspersed with at least 60 seconds at this neutral temperature.

Mild burn injury was induced by delivering a 55 ± 1°C thermal stimulus for 15 seconds using the same stimulation source as all other temperature stimuli. Analysis of oral mucosa and lingual epithelium from injured and uninjured experimental animals showed overt no signs of damage to the tissue. Pharmacological agents were applied by bolus injection of 5ml of drug suspended in water (5mM capsaicin, 10% Menthol or 1.25% allyl isothiocyanate, Sigma) into the oral cavity. An equal volume of vehicle (2% or 5% ethanol) was applied prior as a control for response to drug application. JNJ-17203212 (Sigma) was injected intraperitoneally at 40mg/kg to antagonize TrpV1 channel function.

Imaging data was obtained using an Evolve 512 EMCCD camera. All images were acquired at 5Hz, either at 4x magnification for sparsely expressing GCamp5 lines (TrpA1, Trpm8) or at 10x magnification for densely expressing lines (TrpV1, Wnt1, ΔRosa26^{GCaMP}). A single field of view was analyzed for each experimental animal.

Calcium imaging data collection and analysis

Imaging data was analyzed using custom software implemented in Matlab (MathWorks). For each field of view, all image stacks were first registered for motion correction(Image stabilizer (Li, 2008)). To identify neurons, maps of peak activity (maximal pixel intensity over mean pixel intensity) median filtered, thresholded and separated by watershed segmentation to create candidate regions of interest representing active neurons, which were reviewed manually to identify ROIs for all active neurons. Fluorescence traces for each region of interest were normalized to neighbourhood fluorescence intensity (defined as the average intensity within a two cell radius distance of each cell, excluding all other defined ROIs) to correct for neuropil signal. Calcium transients were automatically detected as fluorescence excursions of >7 fold above noise (defined as median average deviation). To ensure signals originated from a single neuron, we examined the correlation of pixels in the neighbourhood of each ROI to each calcium transient, discarding from analysis any neuron contaminated by outside signal.

Whole mount immunofluorescence

Trigeminal ganglia were dissected, fixed in 4% paraformaldehyde in phosphate buffered saline (PBS) for 2 hours, washed in PBS overnight at 4° C, rinsed in PBS with 0.5% Triton X-100 (PBST), incubated with primary antibodies (chicken anti-GFP, Aves Labs, rabbit anti-CGRP, Immunostar) at 1:500 in blocking solution (PBST, 20% dimethylsolfoxide, 5% goat serum) for 48 hours, washed in PBST, incubated with secondary antibodies (anti-chicken 488, anti Rabbit-546, Invitrogen) at 1:500 in blocking solution overnight, and washed again in PBST.

Behavioral assay for sensitization

Mild burn was performed by placing the hind paw, while mice were deeply anesthetized, in a water bath at 55° C for 15 second. Anesthesia was achieved with Avertin (250 mg/Kg). Animals were tested for cold responses prior to injury and 2 hours after injury as previously described(Brenner et al., 2012). Briefly, mice were placed on a glass plate, a cold stimulus (a pellet of dry ice) was applied to the lower side of the plate directly underneath the hindpaw, and latency to paw withdrawal was recorded. No signs of damage to the paw were observed in this injury model, and behavioral sensitivity to hot and cold returned to baseline levels within 48 hours.

Warmth discrimination behavior

Mice were first water-deprived for 24h to motivate drinking behavior. Individual animals were then trained to perform a temperature discrimination task in a 3-port chamber arena (21cm × 19cm), which was contained within a sound-attenuating cubicle (Med Associates). Temperature cues (40° C or 32° C) were randomly applied through a metal spout in the middle port. The spout was attached to a Peltier module, whose temperature was switched between trials by a temperature controller (TE technology Inc.). Each trial began with the shutter opening in the middle port. Mice were given (up to) 30-sec to lick the spout to continue the trial; otherwise it proceeded to the next trial. One second after detecting the first lick, the shutter in the middle port closed; meanwhile the shutters in the left and right ports

opened simultaneously. Mice were given 4-sec to make a left/right choice and obtain water reward. For a given mouse, reward from one side port was assigned for a temperature cue (e.g. left port for 40° C, right for 32° C; or vice versa). On the wrong trials, mice were given 5-sec timeout as penalty. The inter-trial interval was 10-sec. Mice were trained for two sessions per day, with 80–100 randomized trials (30min) per session. For pharmacological experiments, mice were trained until they could effectively discriminate the temperature with ~90% accuracy (over 2–3 weeks). On the day of the experiments, mice were first tested for 40 trials (pre-test). Then, mice were injected intraperitoneally with TRPV1 antagonist (JNJ-17203212, 40 mg/kg) or vehicle (1:4:15 Pharmasolv: Cremaphor: 5% Dextrose). One hour after injection, mice were retested for another 40 trials. During the test period, timeout was removed to avoid possible re-learning. Animals' performance was calculated as the percentage of the correct choice for a given temperature cue.

We note that this assay requires that the animals learn to associate the temperature of the test probe with the proper behavioral response (e.g. right versus left choice), and so it is essential that the assay be performed "before" and "after" inactivation of TRPV1. As such, it is not possible (or even informative) to carry out this kind of experiments in a TRPV1 knockout background. Importantly, analysis of behavioral performance, as defined by the ratio of attempted versus completed trials, revealed no effect of pharmacological treatment on motivation between control (mean 95.3±2.2%) and treated (97.5±1.0%) animals ($p = 0.376$, t-test).

2-plate choice assay

A two choice temperature assay was used to determine thermal preference. Mice were placed in an apparatus that had a fixed reference plate set at 30° C and test plate with a temperature adjusted between 5 and 50° C (Bioseb). Each animal was tested twice for each parameter and mouse position was quantified over 5 minutes using an automated tracking system. Only those assays in which animals sample both plates within the first minute were scored.

Supplementary Material

Refer to Web version on PubMed Central for supplementary material.

Acknowledgments

We particularly thank Youmei Wu and Nick Ryba for the generous gift of Rosa-GCaMP5, and the Janelia Farm Transgenic Core Services for TrpA1-DTR-Cre animals. We thank Nick Ryba for comments and valuable insights, and Marco Gallio, Kristin Scott, and members of the Zuker lab for helpful comments and suggestions. This work was funded in part by support from the Thomson Family Foundation Initiative in Chemotherapy Induced Peripheral Neuropathy and Sensory Neuroscience, and the intramural program at NIDCR (LAP, MAH). CSZ is an investigator of the HHMI and a senior fellow at the Janelia Farm Research Campus.

References

Akerboom J, Chen TW, Wardill TJ, Tian L, Marvin JS, Mutlu S, Calderon NC, Esposti F, Borghuis BG, Sun XR, et al. Optimization of a GCaMP calcium indicator for neural activity imaging. J Neurosci. 2012; 32:13819–13840. [PubMed: 23035093]

Bautista DM, Jordt SE, Nikai T, Tsuruda PR, Read AJ, Poblete J, Yamoah EN, Basbaum AI, Julius D. TRPA1 mediates the inflammatory actions of environmental irritants and proalgesic agents. Cell. 2006; 124:1269–1282. [PubMed: 16564016]

Bautista DM, Siemens J, Glazer JM, Tsuruda PR, Basbaum AI, Stucky CL, Jordt SE, Julius D. The menthol receptor TRPM8 is the principal detector of environmental cold. Nature. 2007; 448:204–208. [PubMed: 17538622]

Brenner DS, Golden JP, Gereau RWt. A novel behavioral assay for measuring cold sensation in mice. PLoS One. 2012; 7:e39765. [PubMed: 22745825]

Caterina MJ, Leffler A, Malmberg AB, Martin WJ, Trafton J, Petersen-Zeitz KR, Koltzenburg M, Basbaum AI, Julius D. Impaired nociception and pain sensation in mice lacking the capsaicin receptor. Science. 2000; 288:306–313. [PubMed: 10764638]

Caterina MJ, Rosen TA, Tominaga M, Brake AJ, Julius D. A capsaicin-receptor homologue with a high threshold for noxious heat. Nature. 1999; 398:436–441. [PubMed: 10201375]

Caterina MJ, Schumacher MA, Tominaga M, Rosen TA, Levine JD, Julius D. The capsaicin receptor: a heat-activated ion channel in the pain pathway. Nature. 1997; 389:816–824. [PubMed: 9349813]

Cavanaugh DJ, Lee H, Lo L, Shields SD, Zylka MJ, Basbaum AI, Anderson DJ. Distinct subsets of unmyelinated primary sensory fibers mediate behavioral responses to noxious thermal and mechanical stimuli. Proc Natl Acad Sci U S A. 2009; 106:9075–9080. [PubMed: 19451647]

Chuang HH, Prescott ED, Kong H, Shields S, Jordt SE, Basbaum AI, Chao MV, Julius D. Bradykinin and nerve growth factor release the capsaicin receptor from PtdIns(4,5)P2-mediated inhibition. Nature. 2001; 411:957–962. [PubMed: 11418861]

Colburn RW, Lubin ML, Stone DJ Jr, Wang Y, Lawrence D, D'Andrea MR, Brandt MR, Liu Y, Flores CM, Qin N. Attenuated cold sensitivity in TRPM8 null mice. Neuron. 2007; 54:379–386. [PubMed: 17481392]

Davis JB, Gray J, Gunthorpe MJ, Hatcher JP, Davey PT, Overend P, Harries MH, Latcham J, Clapham C, Atkinson K, et al. Vanilloid receptor-1 is essential for inflammatory thermal hyperalgesia. Nature. 2000; 405:183–187. [PubMed: 10821274]

Descartes, R.; Clerselier, C.; La Forge, L.; Schuyl, F. L'homme et un Traitté de la ormation du Foetus du Mesme Autheur. Paris: Charles Angot; 1644.

Dhaka A, Murray AN, Mathur J, Earley TJ, Petrus MJ, Patapoutian A. TRPM8 is required for cold sensation in mice. Neuron. 2007; 54:371–378. [PubMed: 17481391]

Evans PJ. Cryoanalgesia. The application of low temperatures to nerves to produce anaesthesia or analgesia. Anaesthesia. 1981; 36:1003–1013. [PubMed: 7316118]

Frank DD, Jouandet GC, Kearney PJ, Macpherson LJ, Gallio M. Temperature representation in the Drosophila brain. Nature. 2015; 519:358–361. [PubMed: 25739506]

Guler AD, Lee H, Iida T, Shimizu I, Tominaga M, Caterina M. Heat-evoked activation of the ion channel, TRPV4. J Neurosci. 2002; 22:6408–6414. [PubMed: 12151520]

Hensel H, Zotterman Y. The persisting cold sensation. Acta Physiol Scand. 1951; 22:106–113. [PubMed: 14933133]

Huang SM, Li X, Yu Y, Wang J, Caterina MJ. TRPV3 and TRPV4 ion channels are not major contributors to mouse heat sensation. Mol Pain. 2011; 7:37. [PubMed: 21586160]

Jordt SE, Bautista DM, Chuang HH, McKemy DD, Zygmunt PM, Hogestatt ED, Meng ID, Julius D. Mustard oils and cannabinoids excite sensory nerve fibres through the TRP channel ANKTM1. Nature. 2004; 427:260–265. [PubMed: 14712238]

Julius D. TRP channels and pain. Annu Rev Cell Dev Biol. 2013; 29:355–384. [PubMed: 24099085]

Karashima Y, Talavera K, Everaerts W, Janssens A, Kwan KY, Vennekens R, Nilius B, Voets T. TRPA1 acts as a cold sensor in vitro and in vivo. Proc Natl Acad Sci U S A. 2009; 106:1273–1278. [PubMed: 19144922]

Knowlton WM, Palkar R, Lippoldt EK, McCoy DD, Baluch F, Chen J, McKemy DD. A sensory-labeled line for cold: TRPM8-expressing sensory neurons define the cellular basis for cold, cold pain, and cooling-mediated analgesia. J Neurosci. 2013; 33:2837–2848. [PubMed: 23407943]

Kwan KY, Allchorne AJ, Vollrath MA, Christensen AP, Zhang DS, Woolf CJ, Corey DP. TRPA1 contributes to cold, mechanical, and chemical nociception but is not essential for hair-cell transduction. Neuron. 2006; 50:277–289. [PubMed: 16630838]

Lewis AE, Vasudevan HN, O'Neill AK, Soriano P, Bush JO. The widely used Wnt1-Cre transgene causes developmental phenotypes by ectopic activation of Wnt signaling. Dev Biol. 2013; 379:229–234. [PubMed: 23648512]

Li, K. The image stabilizer plugin for ImageJ. 2008.

McCoy ES, Taylor-Blake B, Street SE, Pribisko AL, Zheng J, Zylka MJ. Peptidergic CGRP alpha primary sensory neurons encode heat and itch and tonically suppress sensitivity to cold. Neuron. 2013; 78:138–151. [PubMed: 23523592]

McKemy DD, Neuhausser WM, Julius D. Identification of a cold receptor reveals a general role for TRP channels in thermosensation. Nature. 2002; 416:52–58. [PubMed: 11882888]

Mishra SK, Tisel SM, Orestes P, Bhangoo SK, Hoon MA. TRPV1-lineage neurons are required for thermal sensation. EMBO J. 2011; 30:582–593. [PubMed: 21139565]

Palkar R, Lippoldt EK, McKemy DD. The molecular and cellular basis of thermosensation in mammals. Curr Opin Neurobiol. 2015; 34:14–19. [PubMed: 25622298]

Pedersen JL, Kehlet H. Hyperalgesia in a human model of acute inflammatory pain: a methodological study. Pain. 1998; 74:139–151. [PubMed: 9520228]

Peier AM, Moqrich A, Hergarden AC, Reeve AJ, Andersson DA, Story GM, Earley TJ, Dragoni I, McIntyre P, Bevan S, et al. A TRP channel that senses cold stimuli and menthol. Cell. 2002; 108:705–715. [PubMed: 11893340]

Pogorzala LA, Mishra SK, Hoon MA. The cellular code for mammalian thermosensation. J Neurosci. 2013; 33:5533–5541. [PubMed: 23536068]

Proudfoot CJ, Garry EM, Cottrell DF, Rosie R, Anderson H, Robertson DC, Fleetwood-Walker SM, Mitchell R. Analgesia mediated by the TRPM8 cold receptor in chronic neuropathic pain. Curr Biol. 2006; 16:1591–1605. [PubMed: 16920620]

Rothermel M, Ng BS, Grabska-Barwinska A, Hatt H, Jancke D. Nasal chemosensory-stimulation evoked activity patterns in the rat trigeminal ganglion visualized by in vivo voltage-sensitive dye imaging. PLoS One. 2011; 6:e26158. [PubMed: 22039441]

Saito S, Tominaga M. Functional diversity and evolutionary dynamics of thermoTRP channels. Cell Calcium. 2015; 57:214–221. [PubMed: 25533790]

Schepers RJ, Ringkamp M. Thermoreceptors and thermosensitive afferents. Neurosci Biobehav Rev. 2009; 33:205–212. [PubMed: 18761036]

Story GM, Peier AM, Reeve AJ, Eid SR, Mosbacher J, Hricik TR, Earley TJ, Hergarden AC, Andersson DA, Hwang SW, et al. ANKTM1, a TRP-like channel expressed in nociceptive neurons, is activated by cold temperatures. Cell. 2003; 112:819–829. [PubMed: 12654248]

Swanson DM, Dubin AE, Shah C, Nasser N, Chang L, Dax SL, Jetter M, Breitenbucher JG, Liu C, Mazur C, et al. Identification and biological evaluation of 4-(3-trifluoromethylpyridin-2-yl)piperazine-1-carboxylic acid (5-trifluoromethylpyridin-2-yl)amide, a high affinity TRPV1 (VR1) vanilloid receptor antagonist. J Med Chem. 2005; 48:1857–1872. [PubMed: 15771431]

Tan CH, McNaughton PA. The TRPM2 ion channel is required for sensitivity to warmth. Nature. 2016; 536:460–463. [PubMed: 27533035]

Tominaga M, Caterina MJ, Malmberg AB, Rosen TA, Gilbert H, Skinner K, Raumann BE, Basbaum AI, Julius D. The cloned capsaicin receptor integrates multiple pain-producing stimuli. Neuron. 1998; 21:531–543. [PubMed: 9768840]

Vellani V, Mapplebeck S, Moriondo A, Davis JB, McNaughton PA. Protein kinase C activation potentiates gating of the vanilloid receptor VR1 by capsaicin, protons, heat and anandamide. J Physiol. 2001; 534:813–825. [PubMed: 11483711]

Verdugo R, Ochoa JL. Quantitative somatosensory thermotest. A key method for functional evaluation of small calibre afferent channels. Brain. 1992; 115(Pt 3):893–913. [PubMed: 1628207]

Vriens J, Nilius B, Voets T. Peripheral thermosensation in mammals. Nat Rev Neurosci. 2014; 15:573–589. [PubMed: 25053448]

Vriens J, Owsianik G, Hofmann T, Philipp SE, Stab J, Chen X, Benoit M, Xue F, Janssens A, Kerselaers S, et al. TRPM3 is a nociceptor channel involved in the detection of noxious heat. Neuron. 2011; 70:482–494. [PubMed: 21555074]

Xu H, Ramsey IS, Kotecha SA, Moran MM, Chong JA, Lawson D, Ge P, Lilly J, Silos-Santiago I, Xie Y, et al. TRPV3 is a calcium-permeable temperature-sensitive cation channel. Nature. 2002; 418:181–186. [PubMed: 12077604]

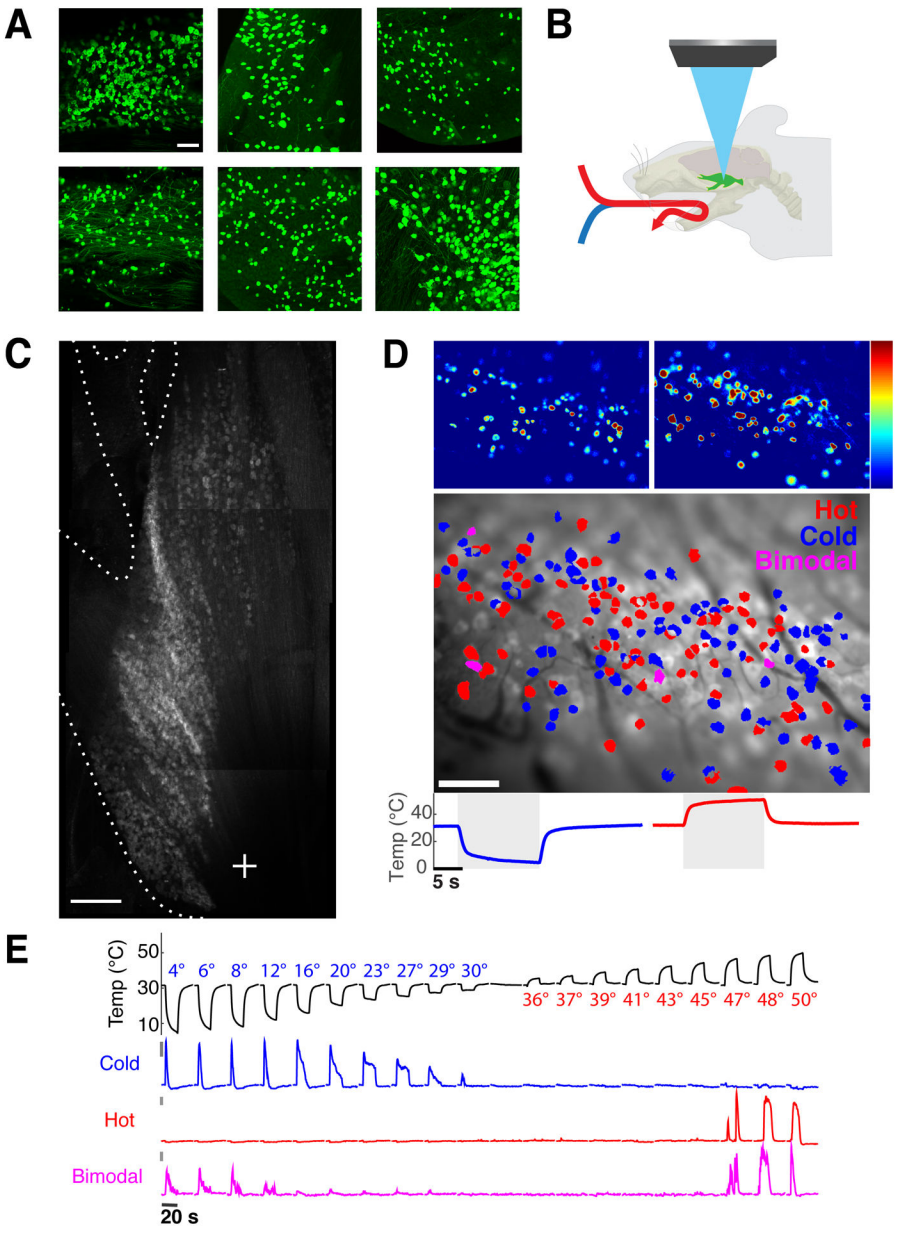

Figure 1. Functional imaging of peripheral thermosensory neurons

A) Shown are whole mount immunofluorescent staining for GCaMP5 in trigeminal ganglia from six driver lines tested for thermosensory sensitivity. Populations labeled by Th^{Cre} and $Parv^{Cre}$ exhibited low-threshold mechanosensory responses but did not respond reliably to thermal stimuli. Scale bar is 100 micron. **B)** Schematic diagram illustrating the methodology employed to record the responses of trigeminal sensory neurons to thermal stimuli (stimuli were applied in the oral cavity. **C)** A top-down view of the trigeminal ganglion imaged at 5x magnification, highlighting the dense fields of neurons (see also Fig S1) and the three branches of the trigeminal nerve (image was obtained using basal GCaMP fluorescence and is a composite of Z-projections through the trigeminal ganglion). Scale bar is 500 micron. **D)** Color-coded heat map of thermosensory responses. The upper left panel shows neurons

responding to cold stimulation, and the right panel those responding to hot stimuli. Shown below the panels are the temperature ramps used for stimulation; color scale indicates percent ΔF/F. The lower panel depicts a color-coded map of the same field, showing distribution of hot, cold, and bimodal thermosensory neurons. Scale bar is 100 micron, color scale indicates maximal percent ΔF/F. **E)** Traces of GCaMP fluorescence changes for three neurons detected in a single imaging field, representing typical response profiles for hot, cold, and bimodal neurons. Bars to left of traces indicate 5% ΔF/F, and the graph above illustrate our standard stimulus series, with a baseline of 32° C and temperature ramps ranging from 4 to 50° C in 19 steps.

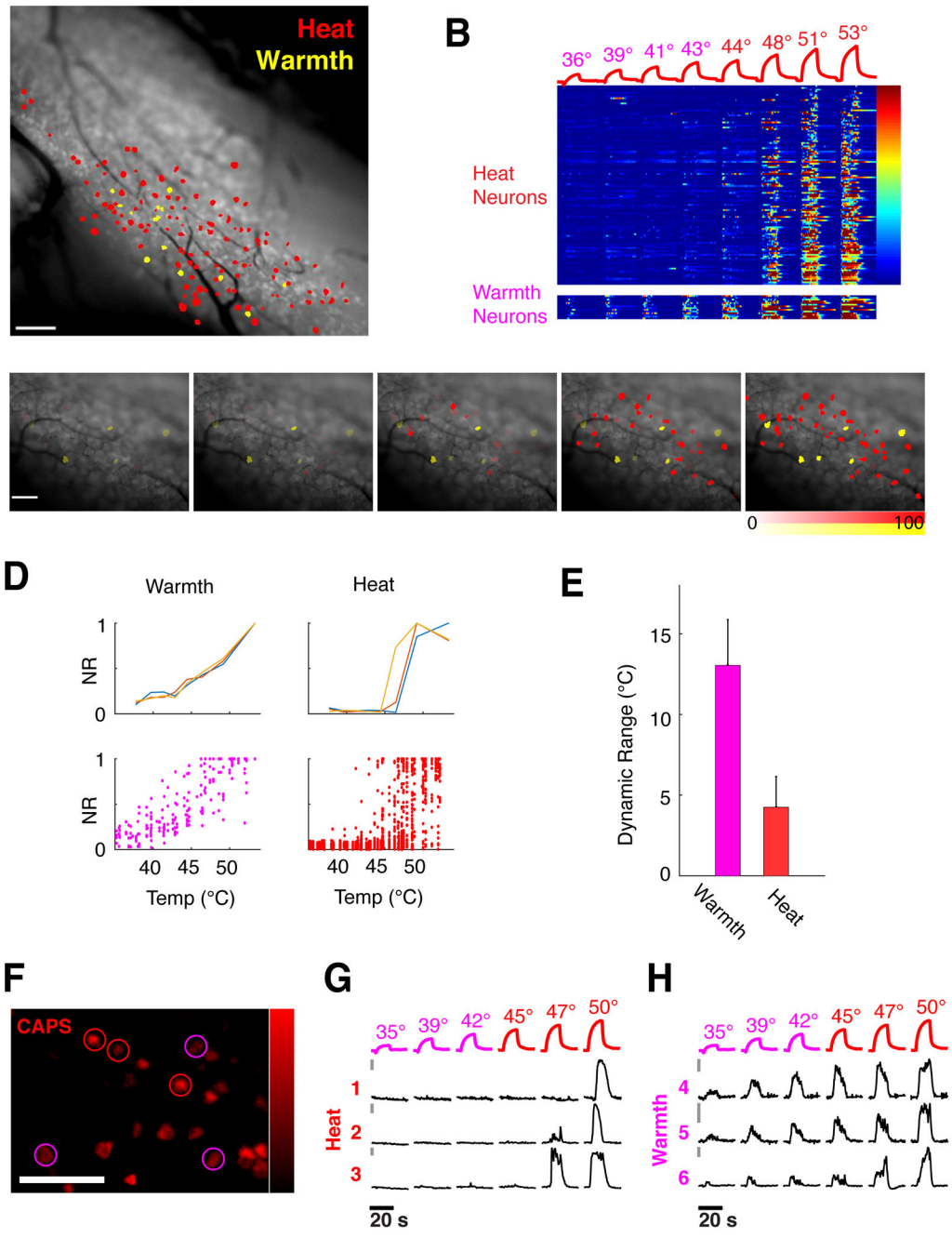

Figure 2. Representation of heat and warmth

A) Composite map of neurons representing heat in a single trigeminal ganglion, labeling the high-threshold noxious heat sensory neurons (red) and the low-threshold warmth sensors (yellow). **B)** Heat map of calcium responses in 122 heat neurons and 14 warm neurons from a single TrpV1^{Cre};Rosa^{GCaMP5} imaging field to a series of heating steps. The vast majority of neurons are only recruited at noxious temperatures. Color scale indicates ΔF/F. **C)** Maps of heat representations in a trigeminal imaging field as a function of temperature. Innocuous temperatures (39° and 42° C) are represented by warm neurons (shown in yellow) while painful heat stimuli recruit a large population of noxious heat neurons (shown in red).

Intensity of labeling indicates normalized calcium response (ΔF/F as percent of maximal response for each neuron). **D**) Temperature coding properties of warmth and heat neurons. Shown above are examples of stimulus- normalized response plots for three warmth sensing neurons (left panel) and three noxious heat neurons (right panel). Lower panels display scatter plots of responses from 22 warm neurons (left) and 187 heat neurons (right) to the same stimulus series. **E**) Warmth neurons encode temperature over a wide dynamic range, defined as temperature differential between 10% and 90% response levels, while heat neurons exhibit much narrower ranges; mean and SEM of dynamic range is plotted for each population. **F–H)** Warmth neurons, like noxious-heat sensors, are activated by capsaicin. Shown in **F** is the population response elicited by capsaicin in a trigeminal imaging field (displayed as maximal projection of ΔF/F after capsaicin stimulation) Warm neurons displayed in panels **G** are circled in magenta, noxious heat neurons in red. **G,H)** Calcium traces of capsaicin-activated warmth and heat cells from panel **C**, cells 1–3 are high-threshold heat neurons, cells 4–6 are warmth-sensing neurons; temperature ramps for stimulation are shown above the traces. Bars (to the left of traces) indicate 5% ΔF/F′; scale bars is 100 micron for all images.

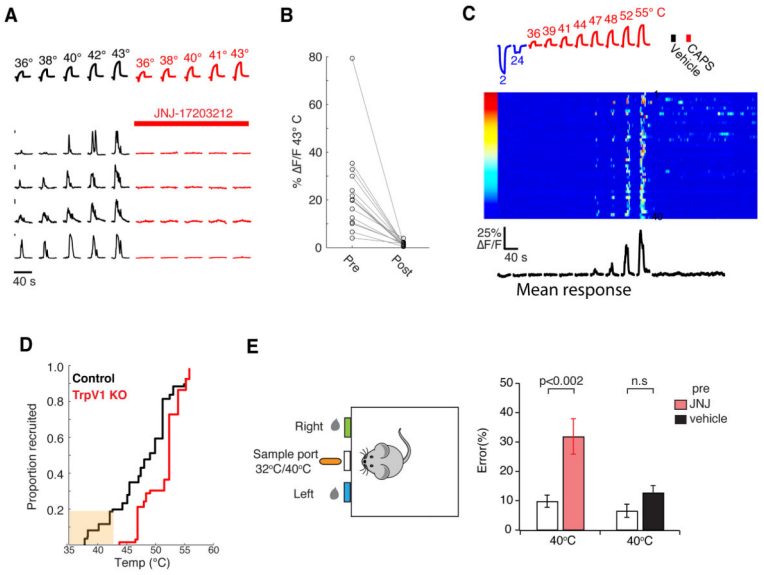

Figure 3. TRPV1 channel is required for warmth sensation

A) Pharmacological inhibition of the TRPV1 ion channel abolishes responses of warm responding neurons to warming stimuli. Shown are responses of four warmth neurons before (left, black traces) and after (right, red traces) blockade of TrpV1 channel with JNJ-17203212. Bars (at left of traces) indicate 5% ΔF/F′. **B)** Quantification of responses before and after administration of JNJ-17203212. For **B,** data are shown for 16 warm sensing neurons from 4 mice. Note the complete loss of responses to the 43° C test stimulus. Recordings from $TrpV1^{Cre}$;$Rosa^{GCaMP5}$ mice; values are maximal ΔF/F. **C)** TrpV1 knockout animals maintain responses to noxious heat (see Fig S6F for responses to cold). Raster plot of 40 heat-responding neurons from a TrpV1 knockout animal to temperatures between 2–55° C (left panel) and to stimulation with 5mM capsaicin (CAPS, right panel). Importantly, while neurons from the TrpV1 knockouts still respond to temperatures above 45° C, they are no longer responsive to capsaicin or innocuous warmth; the traces below show the mean normalized responses from all heat neurons. Color scale indicates percent ΔF/F. **D)** Graph illustrating the cumulative number of neurons responding to increasing temperatures in wild-type (black trace) and TrpV1 KO mice (red trace). Note that warm responding neurons (low-threshold) are missing in the absence of TrpV1 channel. Data were obtained from $\Delta Rosa^{GCaMP}$ mice expressing calcium indicator in all neurons (see Methods), n=3 mice for each genotype. **E)** Pharmacological inhibition of TRPV1 impairs warmth discrimination. Mice trained to associate a warm (40° C) cue with the location of a water reward (top diagram) chose the correct side in ~90% of trials; after pharmacological inhibition of TRPV1, these mice displayed a significant deficit in recognition of the warm stimulus. N =16 mice for inhibition with JNJ-17203212, N=11 for vehicle control, mean and SEM of performance index are plotted for each condition, p-values by Student's T-test. We note that "warmth sensing" also involves cold sensors (Pogorzala et al., 2013), therefore a loss of warm-sensing neurons may not be expected to produce a complete loss of warm detection.

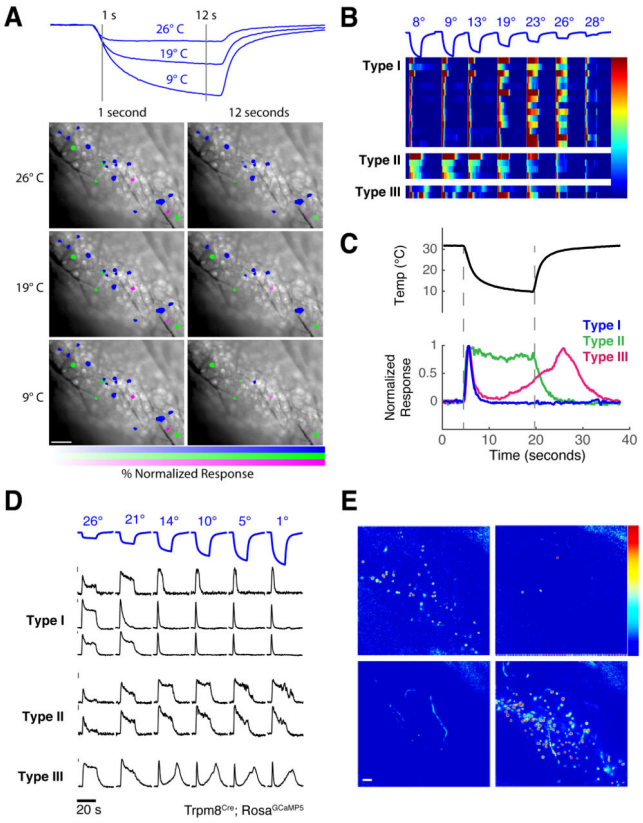

Figure 4. Functional and genetic characterization of cold sensing neurons

A) Calcium imaging of Wnt1^{Cre} and TrpV1^{Cre} (shown here) trigeminal neurons identified three classes of cold-selective responders, color coded within a representative imaging field. Shown are the immediate response to cooling (left panels) and the population response after 12 seconds of stimulus application at 3 different stimulus intensities (9°, 19° and 26° C, stimuli shown above). Intensity of labeling indicates normalized response for each neuron at each temperature and time point (calculated as percentage of maximal calcium response to any cold stimulus). **B**) Heat-map of calcium responses from all cold-sensing neurons labeled in panel **A**, illustrating cold-adapting (Type I) neurons, a smaller population of non-adapting cold neurons (Type II), and a rare subset exhibiting a bi-phasic response (Type III). **C**) Cold sensing neurons exhibit distinct response kinetics, as seen in traces from exemplary neurons of each class. D) Calcium responses from a single Trpm8^{Cre} imaging field, showing that Trpm8^{Cre} neurons represent all three classes of cold sensing neuron. Gray bars represent 5% ΔF/F. All scale bars are 100 microns, color scales represent % ΔF/F. **E)** Maps of GCaMP population responses to intense heating and cooling stimuli show that Trpm8^{Cre} neurons (upper panels) are overwhelming selective for cold stimuli, while the vast majority of Trpa1^{Cre} neurons (lower panels) respond only to heat (see Fig. S8 for quantification).

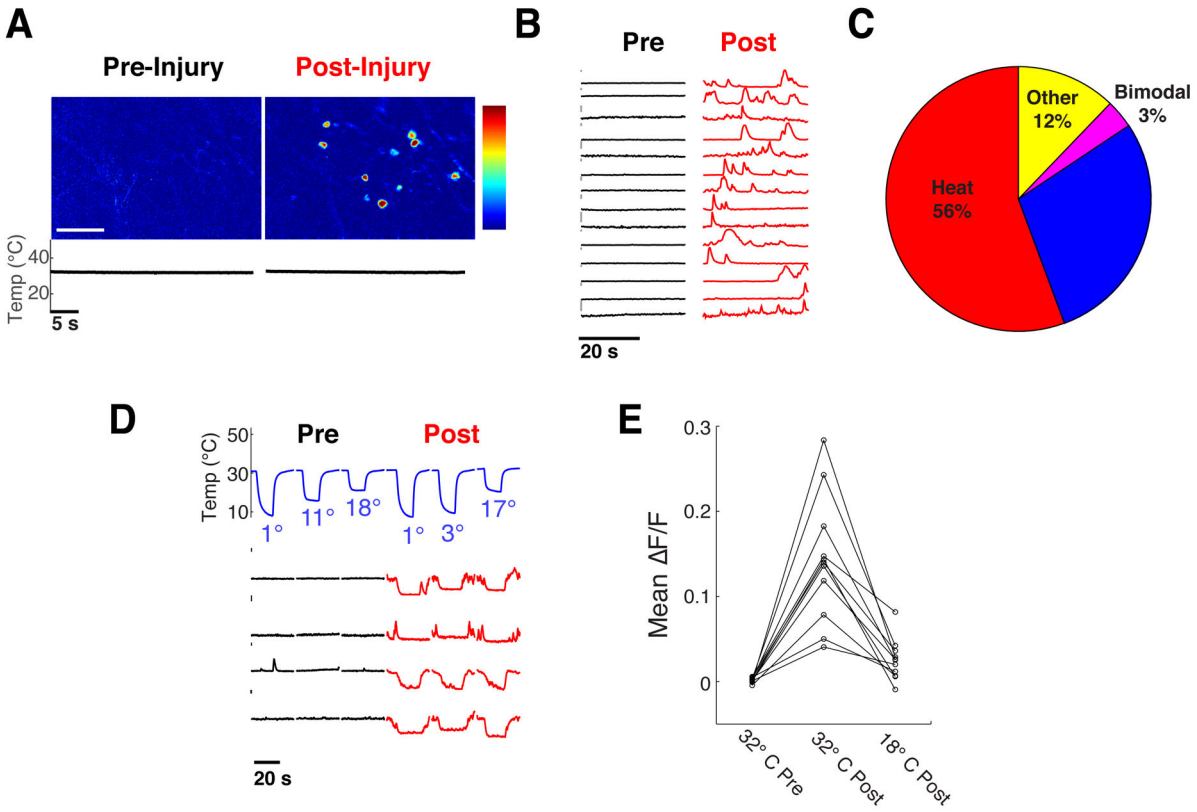

Figure 5. Injury evokes ongoing activity that is suppressed by cooling

A) Left panel shows responses of neurons before injury, and right panel after injury. Temperature was kept constant at 32° C throughout trials; data were obtained from a $TrpV1^{Cre}$;$Rosa^{GCaMP5}$ animal, color scale indicates percent ΔF/F. **B)** Representative calcium imaging traces of neurons from the imaging field shown in panel **A,** illustrating activity while exposed to neutral temperature (32° C). Note that the neurons are silent at neutral temperature before injury but exhibit sporadic episodes of activity after injury. **C)** Distribution of cell types exhibiting spontaneous activity induced by injury. The majority of active neurons were noxious heat sensors, but all thermosensory classes, displayed some degree of spontaneous activity. **D)** Ongoing injury-induced activity can be inhibited by cooling; the spontaneous responses of noxious heat sensors (labeled with GCaMP with the $TrpA1^{Cre}$ driver) after injury can be abolished by brief cooling ramps. Temperature ramps of cooling stimulation are shown above traces; bar to left indicates 5% ΔF/F. **D,E)** Quantification of mean fluorescence in 11 $TrpA1^{Cre}$ labeled neurons from a single imaging field, showing no detectable baseline activity before injury at 32° C, an increase after injury while held at 32° C, and suppression of this activity upon cooling to 18° C.

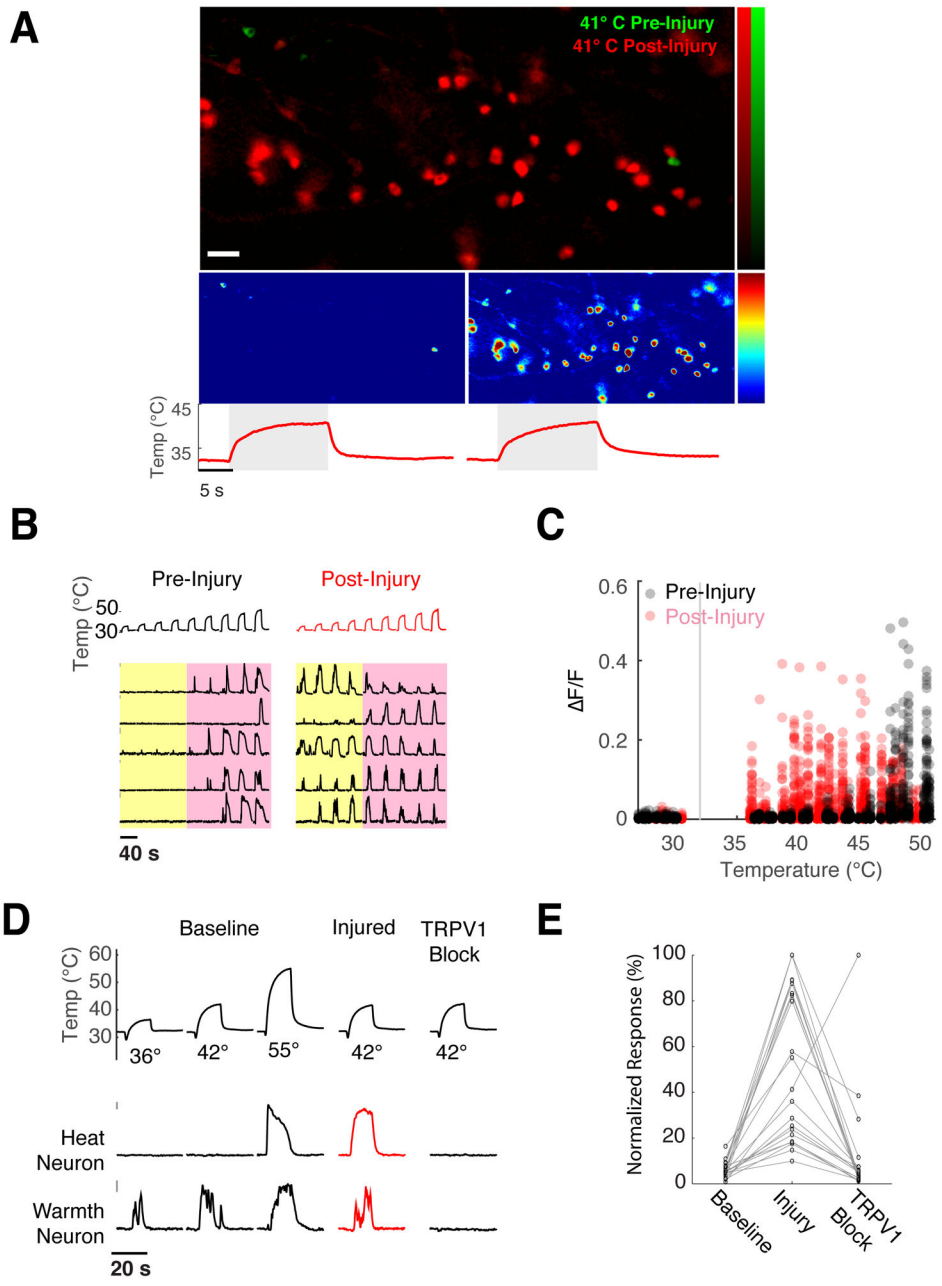

Figure 6. Transformation of heat sensation by injury

A) Injury induces a dramatic recruitment of neurons that now respond to warm temperatures. The upper panel shows a field of neurons stimulated with innocuous warmth (41° C), before (green) and after (red) induction of burn injury (image is an overlay of the maximal projections of GCaMP fluorescence ratio); the panels below show the same field before (left) and after (right) injury. Color scale indicates percent ΔF/F, red traces show the temperature ramps, scale bar is 100 micron. **B)** Representative calcium responses of 5 individual neurons before (left) and after injury (right), demonstrating their profound shift in sensitivity, from the noxious range (>43° C, pink box) to normally innocuous temperatures

(<43° C, yellow box). **C**) Scatter plot of calcium responses for 125 noxious heat neurons before and after thermal injury, illustrating that injury produces a large-scale shift in the thermal sensitivity and preference of this population into the innocuous warm temperature range. **D, E)** Injury induced heat sensitization is dependent on TrpV1. Panel **D** shows representative calcium responses for warmth and noxious heat neurons to mild heating (42°) before injury, after injury, and after subsequent pharmacological inhibition of TRPV1 with JNJ-17203212. Note warmth neuron responses to mild heating are unchanged by injury. Panel **E** shows quantification of sensitization before and after TRPV1 inhibition for all 21 heat neurons tested.

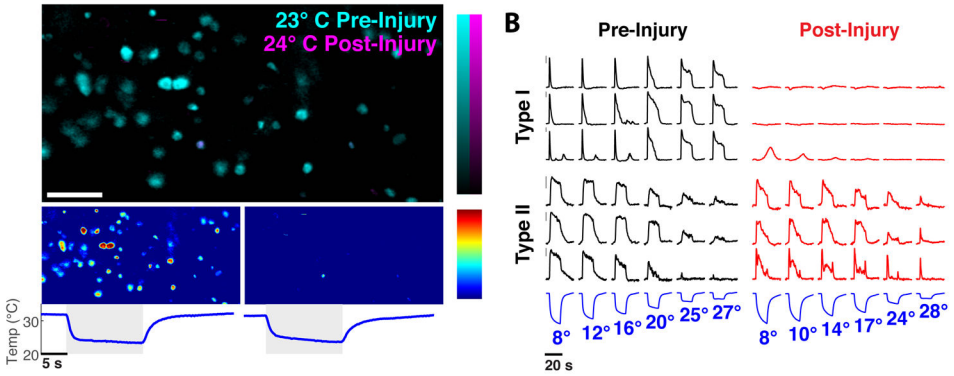

Figure 7. Injury induces the desensitization of innocuous cold neurons

A) Responses to innocuous cold are silenced by injury; upper panel shows neurons activated by moderate cooling before (cyan) and after injury (magenta), lower panels shows responses of the same fields of neurons pre- (left) and post-injury (right); color scales indicate percent ΔF/F, scale bar is 100 μm. **B)** Representative traces of the differential effect of burn injury on the different types of Trpm8-neurons; Type I cold sensors (top traces) exhibit a selective loss of responses. By contrast, the responses of Type II (bottom traces) are largely unaltered. Type III cold neurons (not shown) exhibit desensitization, similar to Type I cells. Temperature ramps of cooling stimuli are shown below traces; bar to left indicates 5% ΔF/F.

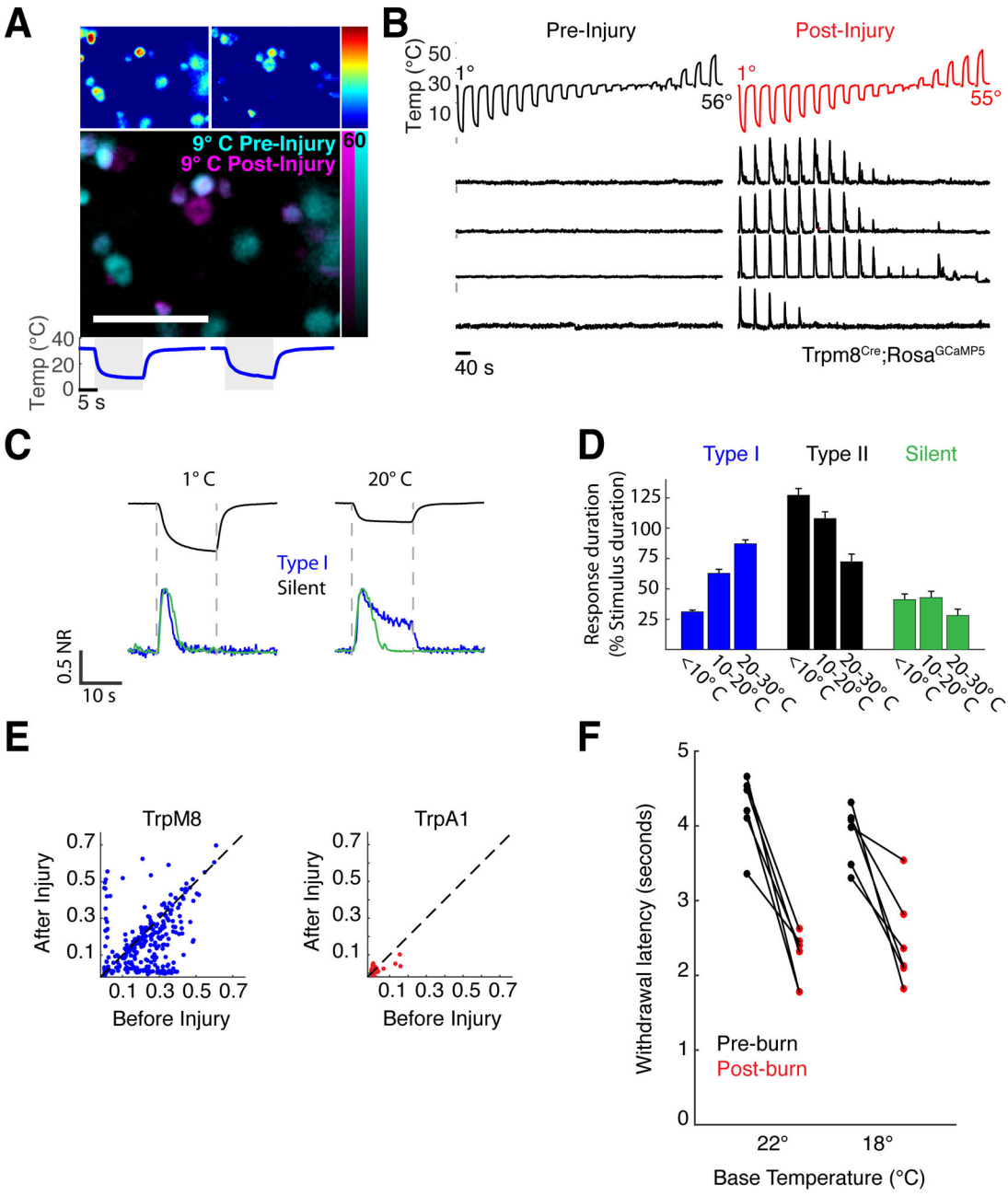

Figure 8. Injury activates a population of silent thermosensory neurons

A) Comparison of population responses to cold reveal a rare class of neurons that are only activated post-injury (white arrowheads). Upper panels shows responses of cold sensitive neurons before (left) and after (right) injury. The lower panel shows the superimposed fields. Pseudo-colored bars to the right indicate percentage ΔF/F; data are from TrpV1^{Cre};Rosa^{GCaMP5} animals. **B)** Representative calcium traces of silent thermosensors demonstrating that these neurons are completely insensitive to a broad temperature range (from 1° to 56° C) prior to injury, yet respond robustly and reliably to cold after injury. Sample data are from a Trpm8^{Cre}; Rosa^{GCaMP5} mouse. **C**) Silent thermosensor cold

responses (green traces) adapt at all stimulus intensities; compare response of a typical silent thermosensor to a Type I cold response (blue traces), which adapts to intense stimuli but sustains during mild cooling. **D**) Quantification of response adaptation as a function of stimulus intensity for Type I, Type II, and silent cold sensors, expressed as duration of the response divided by duration of the cooling stimulus, mean and SEM plotted. **E)** Scatter plots of cold responses (ΔF/F) before and after injury for $Trpm8^{Cre}$ neurons (N = 289 neurons) and $TrpA1^{Cre}$ expressing neurons (N = 153 neurons). Analysis was performed on the maximal calcium responses to noxious cold stimuli (~4° C) before and after injury. Note that responses of silent cold-thermosensory cells are clustered along the y-axis. There are no $TrpA1^{Cre}$-neurons sensitized to noxious cold after injury. **F)** Burn enhances behavioral sensitivity to cooling. Plotted are the latencies of paw reflex withdrawal to a cooling stimulus, before and after injury for 6 mice tested at two baseline temperatures (18°, p=0.0052 and 22° C, p=0.0008, paired Student's T-test).